Bone Morphogenetic Protein (BMP) signaling upregulates expression of the E protein repressors, ID1 and ID3, in pancreatitis and pancreatic ductal adenocarcinoma

Megha Raghunathan[1], Kathleen Scully[1], Amanda Wehrmaker[1,2], Andrew M. Lowy[3], Kathleen E. DelGiorno[4], Pamela Itkin-Ansari[1‡]

[1] Development, Aging and Regeneration Program, Sanford Burnham Prebys Medical Discovery Institute, La Jolla, California, USA.
[2] California State University San Marcos, California Institute for Regenerative Medicine Bridges to Stem Cell Research Program, San Marcos, California, USA.
[3] Department of Surgery, Division of Surgical Oncology, Moores Cancer Center.
[4] Epithelial Biology Center, Vanderbilt University School of Medicine, Nashville, Tennessee; Department of Cell and Developmental Biology, Vanderbilt University, Nashville, Tennessee; Vanderbilt Ingram Cancer Center, Nashville, Tennessee; Vanderbilt Digestive Disease Research Center, Vanderbilt University Medical Center, Nashville, Tennessee.
‡ Correspondence: Pamela Itkin-Ansari, pitkin@sbpdiscovery.org

Abstract

Identification of biological modulators of pancreatic ductal adenocarcinoma (PDAC) initiation and progression are of critical importance as it remains one of the deadliest cancers. We have previously shown that ID1 and ID3 are highly expressed in human PDAC and function to repress expression of E47 target genes involved in acinar cell differentiation and quiescence. More recently, mining of large bulk RNA-seq and single-cell RNA-seq (scRNA-seq) datasets has associated high expression of ID1 with poor PDAC patient survival. Here, we report that BMP2 signaling in human PDAC cells upregulates expression of ID1 and ID3 while treatment with Noggin, an endogenous BMP antagonist, or with DMH1, a selective inhibitor of the BMP receptor, ALK2, reduced expression of ID1/ID3. BMP signaling, working via the canonical pathway involving phosphorylation of SMAD1/5/9 (pSMAD1/5/9), was increased by exogenous BMP2 but blocked by DMH1. Based on immunohistochemical and scRNA-seq analyses, upregulation of BMP signaling and ID1/ID3 also occurs in murine models of pre-neoplastic lesions (KC mice) and pancreatitis induced by the cholecystokinin analog caerulein. Moreover, we demonstrate that BMP dependent ID1/ID3 expression occurs in a non-transformed human ductal cell line. Strikingly, even short term caerulein treatment promoted BMP signaling and ID1/ID3 expression in a rat exocrine cell line, consistent with a direct link between inflammation of the exocrine pancreas and BMP/ID signaling. Together, the data suggest that BMP signaling through pSMAD1/5/9 to ID1 and ID3 occurs early in pancreas pathogenesis and that pancreatic cancer cells remain addicted to this important signaling circuit. Future exploration of druggable targets within this pathway could be of therapeutic benefit in the treatment of pancreatitis and PDAC.

Introduction

ID (inhibitor of differentiation and DNA-binding) proteins (ID1-ID4) are a family of helix-loop-helix (HLH) proteins whose primary function is to prevent basic helix-loop-helix (bHLH) transcription factor dimers from binding to their target genes. Structurally, ID proteins contain a helix-loop-helix (HLH) domain but lack a DNA binding domain, thus sequestering bHLH proteins in non-functional ID/bHLH dimers.

High levels of ID1 and/or ID3 are associated with a variety of cancers, including ovarian cancer, thyroid cancer, and glioblastoma [1-3]. ID proteins promote DNA replication and cell survival and can subvert KRAS-induced senescence [4].

We and others showed that human and murine PDAC cells express ID1 and ID3 and that knockdown reduced cell growth [5-11]. We also demonstrated that ID3 overexpression was sufficient to induce cell cycle entry in normally quiescent human acinar cells, a cell of origin for PDAC[6]. Mechanistically, we found that ID1 and ID3 bind to the bHLH protein E47 (E2A) in PDAC which resulted in suppression of E47 target genes involved in acinar cell differentiation and quiescence [7]. Important questions remain about how ID1 and ID3 are induced in PDAC. Moreover, because protein-protein interactions, e.g. ID/E47, are notoriously difficult to target pharmaceutically, it is critical to identify potentially druggable pathways that impinge on ID1/ID3 expression in PDAC.

Bone morphogenic proteins (BMPs) belong to the transforming growth factor-β (TGF-β) superfamily. This is a large group of structurally related signaling proteins including soluble BMP ligands. These ligands bind to specific BMP type I receptors ALK1 (ACVRL1), ALK2 (ACVR1), ALK3 (BMPRIA), or ALK6 (BMPRIB) that heterodimerize with and phosphorylate one of three BMP type II receptors (ActRII, ActRIIB or BMPR2). In canonical BMP signaling, the activated ALK1/2/3/6 receptors phosphorylate R-SMAD1/5/9 proteins that form a complex with SMAD4 to enter the nucleus and act as a DNA sequence-specific transcription factor complex to regulate transcription of target genes.

In this study, we investigate the relationship between BMP signaling and expression of ID1 and ID3 in diseased pancreatic epithelial cell populations using data from human patients and human PDAC samples as well as mouse tissue, and human and rat cell lines. We also examined earlier stages of pancreas pathogenesis in preneoplastic PanIN lesions and chronic pancreatitis, itself a major risk factor for PDAC. Overall, the data reveal a highly conserved BMP-stimulated increase in ID1 and ID3 expression that occurs at every stage of pancreatic disease and is correlated with poorer outcomes for patients.

Results

Previously, we and others showed upregulation of ID1 and ID3 protein in immunostained human PDAC tissue samples[5-8]. Analysis of numerous published large-scale bulk RNA profiling studies that compared hundreds of human PDAC tumors to normal pancreas or tumor adjacent pancreas tissue allowed us to ask focused questions about the expression of ID1 and ID3 mRNA. Comparison of ID1 and ID3 expression in

normal vs PDAC cells revealed statistically significant increases in ID1 and ID3 mRNA in PDAC compared to normal samples in all five RNA-seq datasets examined (GSE16515, GSE28735, GSE60979, GES62452, CPTAC)[12-16]. The number of normal samples in each dataset ranged from 12-61 and the number of PDAC samples from 36-140. In all five datasets, the difference between the means for normal and PDAC was greater for ID1 than ID3 **(Fig. 1A).** In contrast to IDs, the level of E2A in 5 datasets was not consistently up or downregulated in PDAC, supporting our previous findings that E2A is primarily dysregulated at the level of function, not expression **(Supp Fig. 1).**

To identify specific cell populations within tumors that expressed ID1 and ID3, we interrogated an existing scRNA-seq dataset comprising 24 PDAC tumor samples and 11 control pancreata [17]. The published analysis showed that acinar and type 1 ductal cell populations were present as expected in the normal samples. PDAC tumors also contained type 1 ductal cells, but computational analysis revealed that this population differed from that in normal tissue. In PDAC, type 1 ductal cells were enriched for genes associated with disease related terms, e.g. inflammatory response, cell adhesion and migration. Strikingly, unlike normal samples, PDAC tissue also contained a unique ductal cell type 2 population that was enriched for cancer-related functions, such as cell proliferation, migration, and hypoxia. In addition, ductal type 2 cells had higher expression of CEACAM1/5/6 and KRT19 which are markers associated with poor prognosis in PDAC [17].

Our independent analysis of the aforementioned scRNA-seq dataset identified the same nine clusters in normal samples - acinar, type 1 ductal, endocrine, fibroblast, stellate, B cell, T cell and macrophage populations - and an additional tenth cluster of type 2 ductal cells in PDAC samples **(Fig. 1B)** [17]. Our UMAP computational analysis confirmed the close biological/lineage relationship of the ductal type 1 and ductal type 2 populations as represented spatially in the graphs of the clusters.

Our analysis showed that ID1 transcripts, and to a lesser degree ID3 transcripts, were present in type 1 ductal cells in normal samples. In PDAC type 1 ductal cells, we observed similar levels of ID1 and ID3 mRNA. In PDAC-specific type 2 ductal cells, however, our analysis showed a significant increase in ID1 transcripts as compared to type 1 ductal cells in either normal or PDAC samples transcripts **(Fig. 1C)**.

We considered whether high expression of ID1 and ID3 was associated with specific PDAC subtypes. Previous work by others using unsupervised clustering of bulk RNA-seq data from 96 human PDAC tumors with high epithelial content (>40%) identified four subtypes of tumors – aberrantly differentiated endocrine/exocrine (ADEX), immunogenic, pancreatic progenitor, and squamous [18]. Using this dataset, we queried expression levels of ID1 and ID3 mRNA in each of the four PDAC subtypes. For ID1, significantly higher expression was observed in the squamous subtype than in the immunogenic, pancreatic progenitor, or ADEX subtypes. For ID3, high expression was more closely associated with the squamous, pancreatic progenitor and immunogenic subtypes than the ADEX subtype **(Fig. 2A)**.

Previous survival analysis of 93 patients stratified by PDAC subtype showed median survival of 25.6 months with ADEX, 30 months with immunogenic, 23.7 months with pancreatic progenitor and only 13.3 months for patients with the squamous subtype of tumor [18]. Separately, we carried out survival analysis for

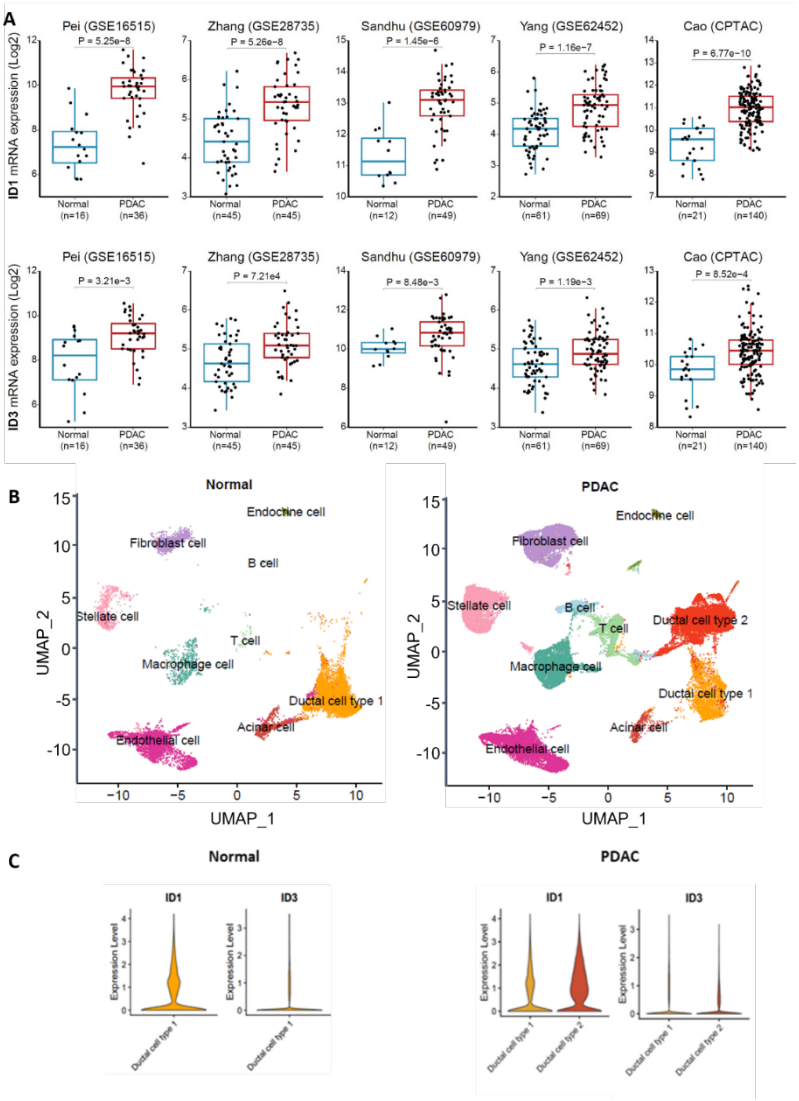

Fig. 1: ID1 and ID3 are highly expressed in human PDAC.

(A) ID1 and ID3 RNA expression from five independent data sets profiling bulk RNA expression from human normal and PDAC tissue. GSE16515, GSE28735, GSE60979, GSE62452 are microarray analyses. CPTAC (NCI Clinical Proteomic Tumor Analysis Consortium) is RNA-seq analysis. P values were determined by Wilcoxon Rank Sum test **(B)** UMAP analysis of existing scRNA-seq data from 11 normal and 24 human PDAC samples (Peng et al Cell Research 2019, Genome Sequence Archive CRA001160) **(C)** Violin plots of ID1 and ID3 RNA expression in ductal cell type 1 in normal samples (left) compared to PDAC ductal cell type 1 and type 2 cells (right) (Peng et al Cell Research 2019, Genome Sequence Archive CRA001160).

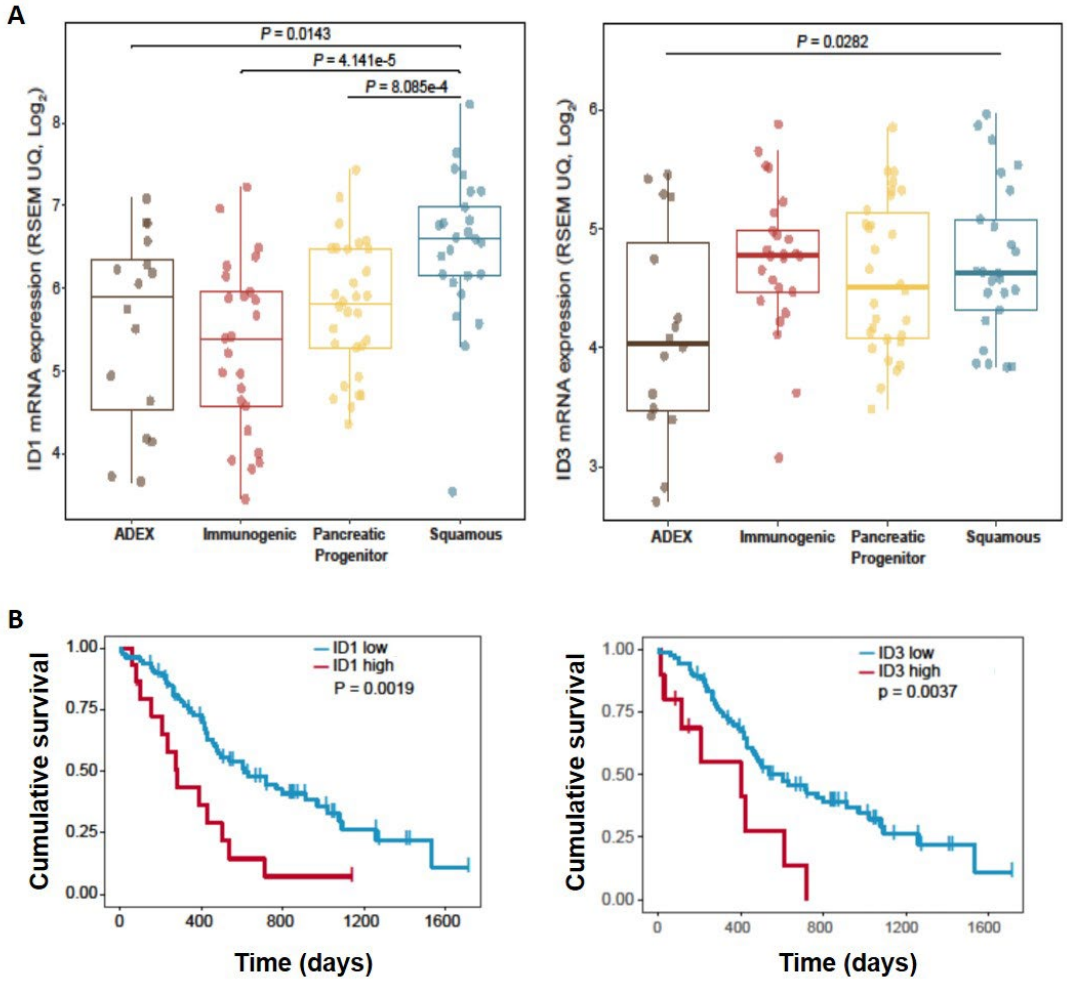

Fig. 2: High expression of ID1 and ID3 is associated with poor patient survival.

(A) Expression of ID1 and ID3 RNA in four PDAC subtypes. The RNA-seq data that identified the four subtypes was generated from bulk RNA extracted from 96 human tumors with high epithelial content (≥40%) (Bailey et al Nature 2016, https://dcc.icgc.org/repositories under the identifier PACA-AU). These same four subtypes were also identified in 232 pancreatic cancers using array-based mRNA expression profiles encompassing the full range of tumor cellularity (from 12–100%). ADEX is aberrantly differentiated endocrine exocrine **(B)** Kaplan-Meier survival analysis of patients stratified by expression level of ID1 and ID3 RNAs (Bailey et al Nature 2016, https://dcc.icgc.org/repositories under the identifier PACA-AU). Median survival was estimated using the Kaplan-Meier method and the difference was tested using the log-rank test. P values <0.05 were considered statistically significant.

patients stratified by high versus low expression of ID1 and ID3 mRNA. For both ID1 and ID3, high expression was correlated with shorter survival time from diagnosis. Patients with high ID1 expressing tumors showed median survival of 300 days versus those with low ID1 expressing tumors who had median survival of 650 days. The difference was smaller for ID3 where patients with high ID3 expressing tumors had median survival of 400 days versus those with low ID3 expressing tumors who had median survival of 600 days **(Fig. 2B)**.

Given that BMP signaling has been shown to upregulate ID1 and ID3 gene expression in multiple tissues and having established that upregulation of ID1 and ID3 in PDAC tumors is associated with shorter patient survival times following diagnosis, we considered that expression of ID1 and ID3 might be regulated by BMP signaling in PDAC. To investigate this, we examined the expression of BMP1, BMP2, BMP4 and the Type II receptor BMPR2 in the same five datasets previously examined above for ID1 and ID3 expression in Fig. 1A [12-16]. BMP1 and BMP2 were upregulated in PDAC tumor tissue relative to normal samples in three out of five and two out of five datasets, respectively. Strikingly, however, BMP4 and BMPR2 were significantly upregulated in the tumor samples from all five datasets (**Fig. 3A)**.

Consistent with the finding that BMP4 and BMPR2 are the most highly expressed BMP signaling molecules in PDAC tumors in the bulk RNA-seq analyses, analysis of the Peng et al., scRNA-seq dataset also showed upregulated expression of BMP4 and BMPR2 in the type 2 ductal cell population specific to PDAC as compared to the type 1 ductal cell populations in normal or PDAC tissue **(Fig. 3B)** [17]. Altogether, the cell population identified to have the highest expression of ID1 and ID3 also has the highest expression of BMP4 and BMPR2 and in PDAC specific type 2 ductal population.

High levels of BMP4 and BMPR2 mRNA observed in the type 2 ductal cell population led us to examine SMAD signaling activity in PDAC lesions in human patient samples. A primary measure of active BMP signaling is nuclear localization of phosphorylated SMAD1/5/9 proteins (pSMAD1/5/9). Immunostaining of human PDAC tissue from four patients revealed nuclear pSMAD1/5/9 in the lesions of diseased pancreata, providing evidence of active BMP signaling in all four patient samples **(Fig. 3C)**. In addition to human PDAC tissue and cell lines, we examined tissue from the *LSL-Kras*$^{G12D/+}$*;Trp53*^{R172H}*;Pdx1Cre* (KPC) mouse model of pancreatic cancer which faithfully recapitulates human PDAC development. Tissue from 3-month old mice harbored primarily PanIN lesions and these exhibited nuclear pSMAD1/5/9. **(Supp Fig. 2A)** [19].

To investigate a functional relationship between BMP signaling and expression of ID1 and ID3 in PDAC, two PDAC cell lines were utilized: PANC-1 and 779e. The latter is a patient-derived cell line from a primary PDAC that we recently described [20,21]. Both PANC-1 and 779e cell lines harbor oncogenic mutations in *KRAS* and loss-of-function mutations in *TRP53*. They also lack expression of p16^{INK4a}/CDKN2A but retain expression of SMAD4 [21].

As a first test of active BMP signaling, PANC1 and 779e cells were treated with Noggin, which binds to BMPs preventing receptor binding. Noggin treatment lowered ID1 and ID3 mRNA expression **(Fig. 4A)**. In contrast, treatment with recombinant BMP2 for 3 hours increased levels of pSMAD1/5/9 protein and

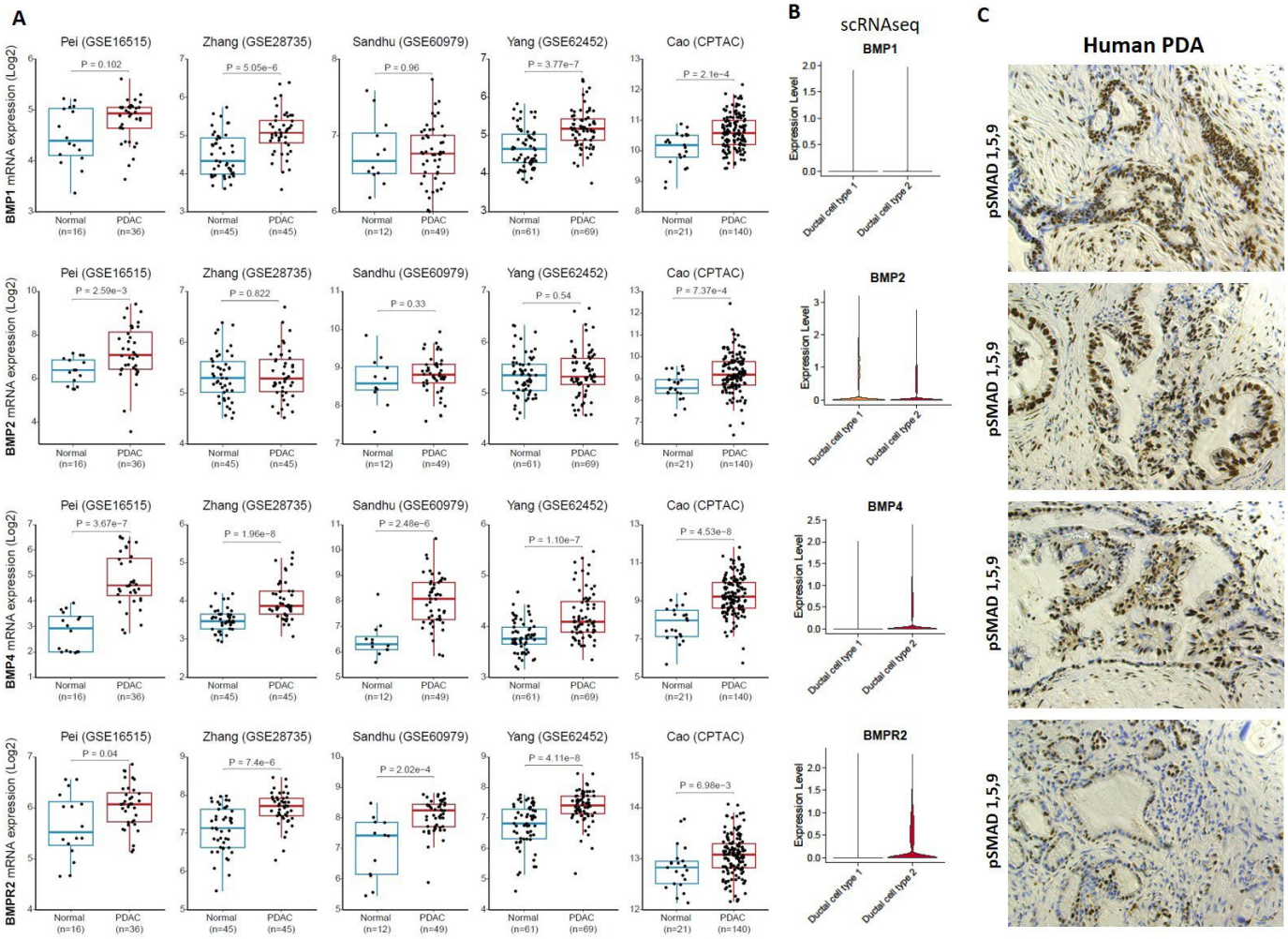

Fig. 3: BMP signaling is upregulated in human PDAC.

(A) Expression of RNA encoding BMP1, BMP2 and BMP4 ligands and BMPR2 receptor from five independent data sets profiling bulk RNA expression from human normal and PDAC tissue. GSE16515, GSE28735, GSE60979, GSE62452 are microarray analyses. CPTAC (NCI Clinical Proteomic Tumor Analysis Consortium) is RNA-seq analysis. P values were determined by Wilcoxon Rank Sum test. **(B)** scRNA-seq data from 24 human PDAC samples (Peng et al Cell Research 2019, GSA CRA001160). Expression of BMP1, BMP2 and BMP4 ligands and BMPR2 receptor RNA in ductal cell type 1 in normal samples compared to PDAC ductal cell type 1 and type 2. **(C)** pSMAD 1/5/9 immunostained four human PDAC patient FFPE tissue samples, 200x.

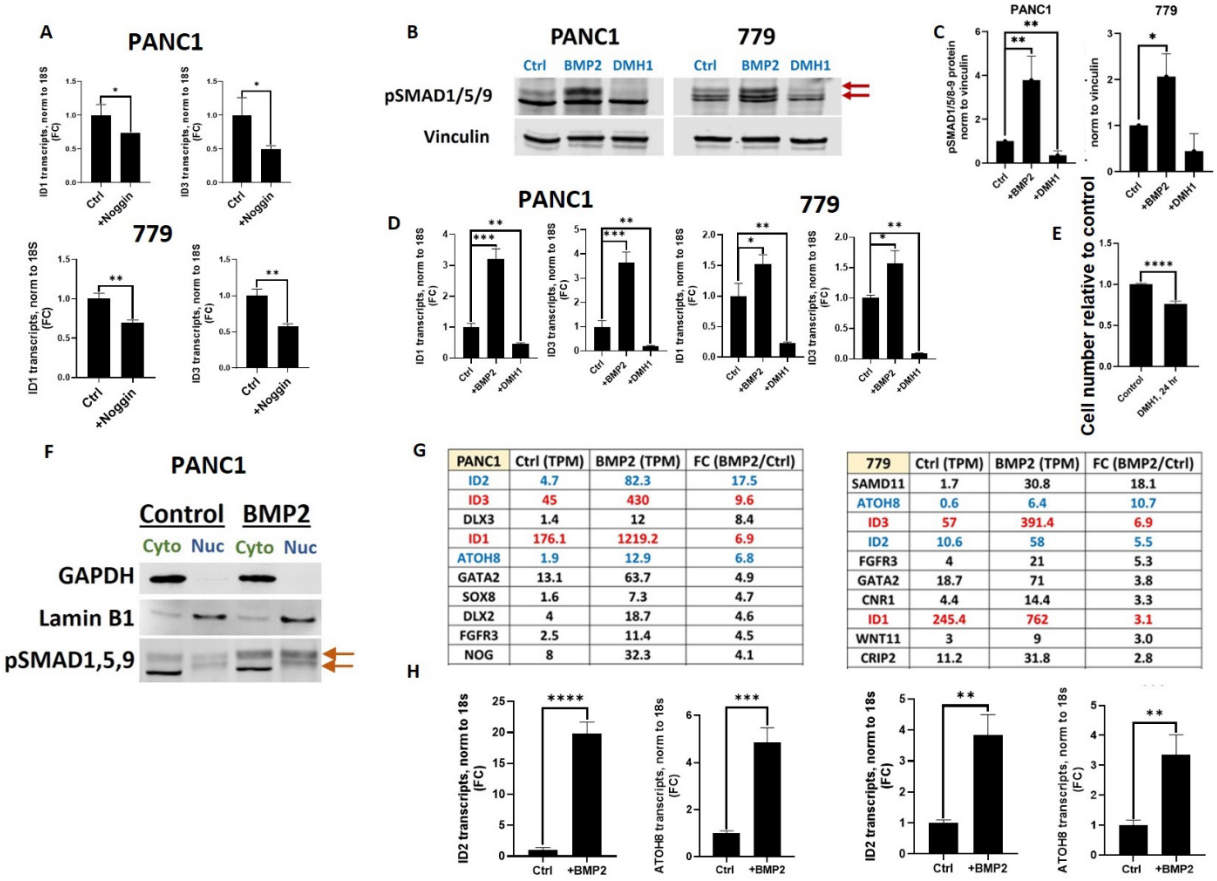

PANC1	Ctrl (TPM)	BMP2 (TPM)	FC (BMP2/Ctrl)
ID2	4.7	82.3	17.5
ID3	45	430	9.6
DLX3	1.4	12	8.4
ID1	176.1	1219.2	6.9
ATOH8	1.9	12.9	6.8
GATA2	13.1	63.7	4.9
SOX8	1.6	7.3	4.7
DLX2	4	18.7	4.6
FGFR3	2.5	11.4	4.5
NOG	8	32.3	4.1

779	Ctrl (TPM)	BMP2 (TPM)	FC (BMP2/Ctrl)
SAMD11	1.7	30.8	18.1
ATOH8	0.6	6.4	10.7
ID3	57	391.4	6.9
ID2	10.6	58	5.5
FGFR3	4	21	5.3
GATA2	18.7	71	3.8
CNR1	4.4	14.4	3.3
ID1	245.4	762	3.1
WNT11	3	9	3.0
CRIP2	11.2	31.8	2.8

Fig. 4: BMP signaling to IDs is blocked by Noggin and DMH1.

(A) RT-qPCR of ID1 and ID3 in PANC1 and 779 cells treated with the BMP antagonist Noggin **(B)** Western blot analysis of protein extracts from PANC1 and 779e cell lines following treatment with BMP2 ligand or DMH1, a highly selective small molecule BMP inhibitor which is an antagonist of the ALK2 receptor. **(C)** Relative quantitation of pSMAD1/5/9 compared to vinculin controls in Western blots shown in Fig. 4B using ImageJ (http://rsb.info.nih.gov/ij/). **(D)** qPCR quantitation of ID1 and ID3 RNA in human PANC1 and 779e cells following treatment with BMP2 or DMH1. Values were normalized to 18 rRNA. **(E)** PANC1 viable cell number relative to control following 24-hour treatment with DMH1. Cell count is based on Alamar Blue staining measured at 590nm. **(F)** Western blot analysis of cytoplasmic versus nuclear fractions of protein extracts from PANC1 cells following treatment with BMP2 ligand. GAPDH as a control for cytoplasmic fraction and Lamin B1 as a control for the nuclear fraction **(G)** The ten most highly upregulated genes in PANC1 and 779e cells following treatment with BMP2 from RNA-seq data. **(H)** qPCR verification of RNA-seq data shown in Fig. 4E for ID2 and ATOH8 RNA from PANC1 and 779e cells.

stimulated expression of ID1 and ID3 mRNA in both PANC-1 and 779e cells **(Fig. 4B-D)**. Treatment with the dorsomorphin analog DMH1, a highly selective small molecule antagonist of the BMP receptor ALK2 (*ACVR1* gene) decreased levels of pSMAD1/5/9 protein and ID1 and ID3 mRNA **(Fig. 4B-D)** [22,23]. Moreover, 24-hour treatment with DMH1 resulted in 20% fewer cells relative to control cultures **(Fig. 4E)**. Consistent with canonical BMP signaling in PANC1 and 779e cells, cytoplasmic and nuclear fractions of BMP2 treated PANC1 cells revealed that BMP2 induced not only higher levels of pSMAD1/5/9, but also its translocation from cytoplasm to nucleus **(Fig. 4F)**.

Having shown that BMP2 upregulates expression of ID1 and ID3 mRNA, we next sought to identify where ID1 and ID3 ranked in the hierarchy of BMP targets genes. PANC1 and 779e cells were treated +/- BMP2 for 3 hours, followed by isolation of mRNA for RNA-seq. Strikingly, the data showed that ID1 and ID3 mRNA were in the top ten BMP2-induced genes based on fold-change as well as TPM (transcripts per million). In addition to ID1 and ID3, BMP2 also upregulated ID2, although TPM for ID2 was five to ten-fold lower than ID1 or ID3 in PANC1 and 779e cells at baseline or upon BMP2 induction. BMP2 also induced ATOH8/MATH6 mRNA expression, which codes for a protein involved in pancreas development that functions similarly to ID proteins by forming non-functional dimers with E47 to inhibit E47 target gene activation **(Fig. 4G)** [24]. The RNA-seq data was verified by qPCR of ID2 and ATOH8 **(Fig. 4H)** as we previously showed for ID1 and ID3 **(Fig. 4D)**. Together, the data suggest that a primary function of BMP signaling in PDAC is to disable E47 by means of ID and ATOH8 induction.

Most human PDAC is diagnosed late in its natural history, where we show high levels of pSMAD1/5/9 (**Fig. 3C**). To provide a window into earlier stages of pathogenesis, we examined the *Kras*$^{G12D/+}$*; Pdx1Cre* (constitutive KC) mouse model of PanIN development. KC mice express oncogenic *Kras*^{G12D} in the pancreas, and the lesions that develop closely resemble human PanINs histologically and biochemically [25]. At 3-months, PanIN lesions in KC mice exhibited high levels of pSMAD1/5/9 **(Supp Fig. 2B)**. To interrogate ID1 and ID3 mRNA expression, we investigated scRNA-seq data from *LSL-Kras*$^{G12D/+}$*;Ptf1aCre*$^{ERTM/+}$ (inducible KC mice) [26,27 28]. Several abnormal cell populations (that make up PanIN lesions) were identified including, 'Pit cell-like' (*Muc5ac*+), 'Proliferating Metaplasia', 'Senescent' and 'Tumor', all of which highly expressed both ID1 and ID3 mRNA **(Fig. 5A)**. The data suggest that dysregulation of BMP signaling to IDs occurs early in pathogenesis.

To determine how early in pancreas pathogenesis upregulated BMP signaling and ID1/ID3 expression occur, we examined pancreatitis, a known risk factor for PDAC. The most commonly used mouse model of pancreatitis employs treatment with supramaximal doses of the cholecystokinin (CCK) analog caerulein. Acinar cells respond to caerulein with ER stress and unfolded protein response, along with forced secretion of exocrine digestive enzymes resulting in parenchymal damage [29]. Wild type mice chronically treated with caerulein (2-4 weeks) display significant acinar-to-ductal metaplasia (ADM) comprising heterogeneous epithelial cells, including mucinous/ductal, tuft, and enteroendocrine cell populations [30]. To investigate a role for ID1/ID3 in pancreatitis, we analyzed a scRNA-seq dataset generated from the pancreata of mice treated with caerulein for 2 to 4 weeks. The data revealed that both *Id1* and *Id3* were highly upregulated in the injury-induced mucinous/ductal cell population as compared to acinar cells or other ADM-induced populations **(Fig. 5B)**.

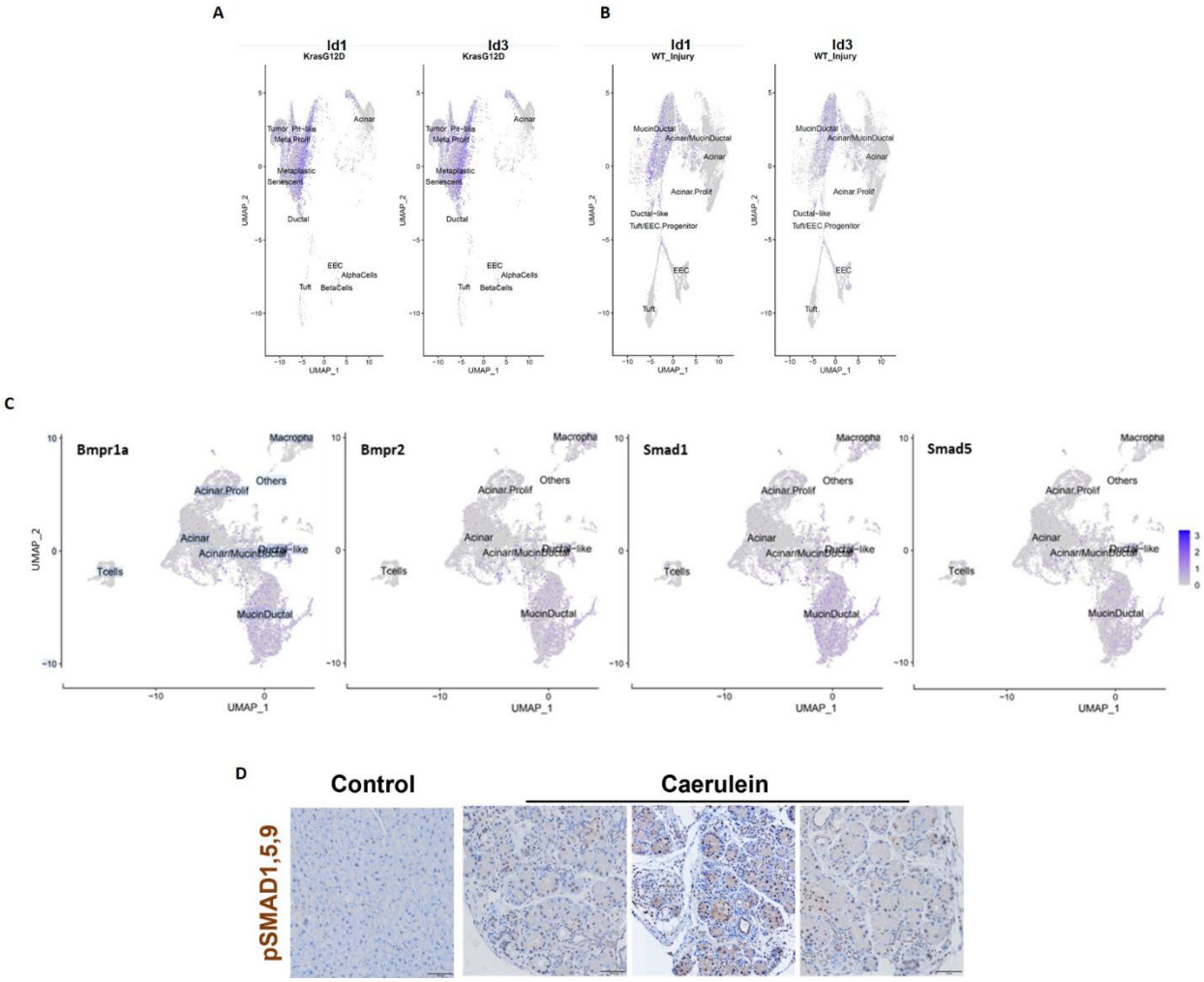

Fig. 5: BMP receptors and SMAD effectors are upregulated in caerulein-induced pancreatitis in the MUCIN/DUCTAL population of cells (product of ADM).

(A) Levels of ID1 and ID3 RNA from scRNA-seq in mice harboring Kras ^{G12D} mutation (Ma DelGiorno Gastro 2022) **(B)** Levels of ID1 and ID3 RNA from scRNA-seq in CD-1 mice following 4 weeks of caerulein treatment (Ma DelGiorno Gastro 2022) **(C)** Levels of Bmpr1a, Bmpr2, Smad1 and Smad5 RNA from scRNA-seq in CD-1 mice following 4 weeks of caerulein treatment (Ma DelGiorno Gastro 2022) **(D)** 4-week caerulein-treated CD-1 mice and control pancreas tissue immunostained for pSMAD1/5/9.

Moreover, *Bmpr2*, *Bmpr1a*, *Smad1* and *Smad5* were also highly expressed in the mucinous/ductal cell populations, suggesting active BMP signaling **(Fig. 5C)**. Consistent with this, immunostaining of tissue from caerulein-treated mice revealed that the injured pancreata exhibited nuclear pSMAD1/5/9 expression, evidence of active, canonical BMP signaling (**Fig. 5D**).

Having shown that caerulein induced BMP signaling and expression of ID1 and ID3 mRNA in murine pancreatitis, we wanted to determine whether this occurred in a cell-autonomous manner or required signaling from neighboring cells. We employed HPNE cells, a non-tumorigenic line derived from hTERT immortalization of human pancreatic exocrine cells, treated with BMP2 or DMH1. Data from Western blot analysis mirrored that of PDAC lines with increased pSMAD1/5/9 in response to BMP2 and decreased pSMAD1/5/9 in response to DMH1 **(Fig. 6A)**. qPCR analysis showed that expression of ID1 and ID3 mRNA also increased in response to BMP2 and decreased in response to DMH1 (**Fig. 6B**). Together, the data support the hypothesis that BMP signaling, response to inhibitors of BMP signaling, and expression of ID1 and ID3 mRNA can occur in a cell autonomous manner prior to tumorigenesis.

The rat acinar cell line AR42J has been widely used to study exocrine pancreas function particularly as an *in vitro* model of caerulein-induced acute pancreatitis [31]. AR42J cells maintain many characteristics of normal pancreatic acinar cells including calcium signaling and synthesis and secretion of digestive enzymes. AR42J cells were treated with caerulein or BMP2, the latter as a positive control. Western blot analysis showed an increase in pSMAD1/5/8 (pSMAD8 is alternate nomenclature for pSMAD9) in response to both caerulein and BMP2 **(Fig. 6D)**. qPCR analysis showed that expression of ID1 and ID3 mRNA also increased in response to both caerulein and BMP2 (**Fig. 6E**). Together the data suggest a circuit in which exocrine cell stress, in this case modeled by 3-hour treatment with caerulein, activates BMP signaling to induce expression of ID1 and ID3 in a cell-autonomous manner.

Discussion

The tumorigenic function(s) of ID proteins in many cancers is well established [32]. Studies from our lab and others have clearly demonstrated that ID proteins play a pathogenic role in PDAC [6,7,9,10]. We and others have also shown that knockdown of ID1 or ID3 decrease PDAC cell viability [6,10]. Our previous work showed that ID1 and ID3 bind to and inhibit the activity of the bHLH transcription factor E47, a splice variant of the *E2A*/*TCF3* gene. Importantly, we found that restoring E47 activity in PDAC induced quiescence and expression of acinar cell differentiation markers *in vitro* and *in vivo* [7,21]. Given the significance of IDs in PDAC, we were interested in what upstream signals might control expression of the ID genes. In many diverse biological processes, it's known that BMP signaling induces expression of ID1 and ID3 [32].

Here, we report that BMP signaling is active in PDAC tumors as evidenced by the high expression of BMP ligands and receptors, and by induction of nuclear pSMAD1/5/9. BMP signaling upregulates expression of ID1 and ID3 which is, in turn, correlated with shorter survival times. We determined that BMP signaling

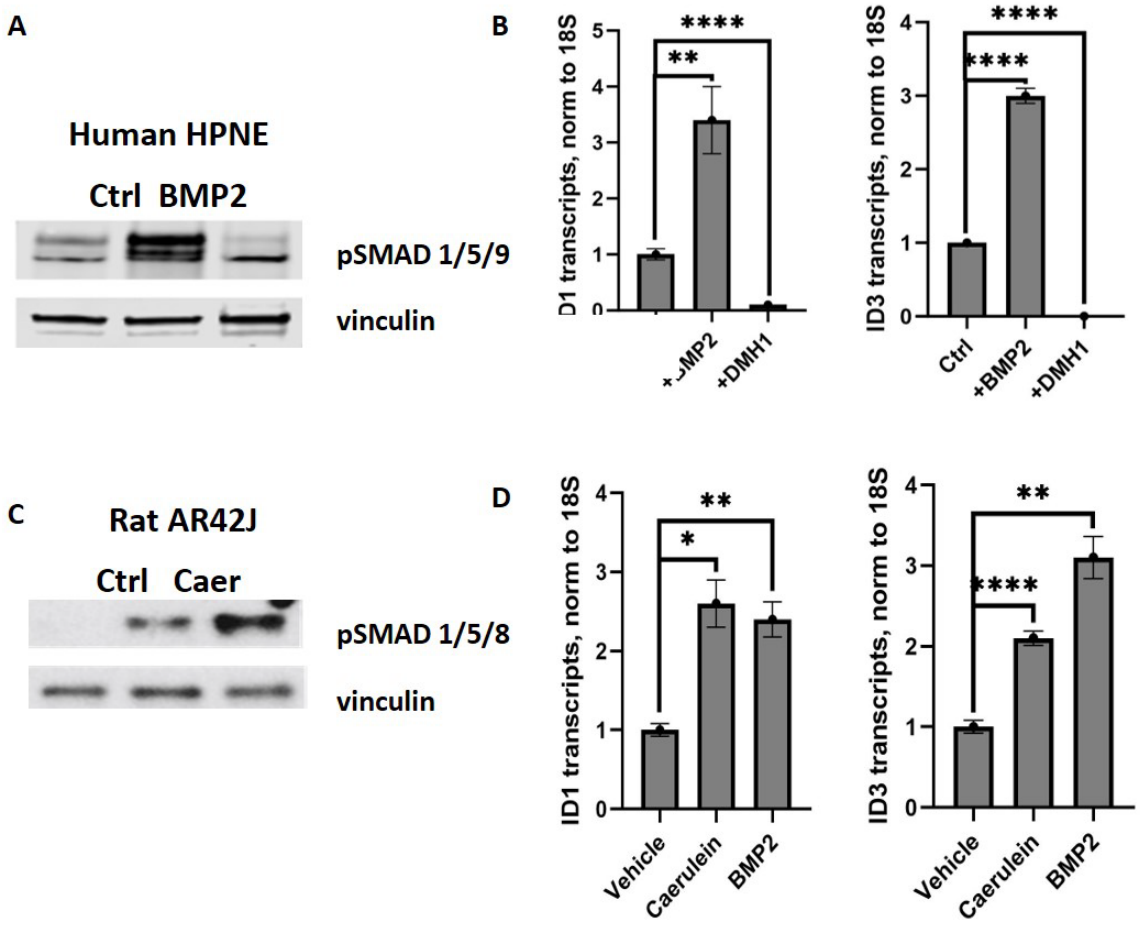

Fig. 6: BMP receptors and SMAD effectors are upregulated in caerulein-induced pancreatitis in the MUCIN/DUCTAL population of cells (product of ADM).

(**A**)Western blot analysis of human HPNE following BMP2 or DMH1 treatment (**B**) RT-qPCR analysis of ID1 and ID3 in HPNE cells treated in 6B. (**C**) Western blot analysis of rat AR42J cells following caerulein or BMP2 treatment (**D**) RT-qPCR analysis of ID1 and ID3 in AR42J cells treated in 6B.

was required for high levels of ID1 and ID3 expression because blocking BMP signaling with either the endogenous antagonist, Noggin, or the small molecule BMP antagonist, DMH1, reduced expression of both ID1 and ID3. In line with the role of IDs in cell cycle, 24 hours of treatment with DMH1 resulted in decreased cell number relative to controls. Conversely, treating cells with recombinant BMP2, which was previously shown to be highly expressed in PDAC, significantly increased expression of ID1 and ID3 indicating that expression in PDAC cell lines is sub-maximal under normal culture conditions [33]. Further, our studies in human tissue and cells, as well as mouse tissue and rat cells, suggest that BMP signaling to IDs in the exocrine pancreas is conserved across species.

In mouse, scRNA-seq of three PDAC GEMMs established the emergence of two cancer cell populations in PDAC progression – one early epithelial ductal cell type 1 population and a second late-stage ductal cell type 2 mesenchymal-like population that developed in the setting of multiple secondary driver mutations. (Hosein Brekken JCI 2019). In separate work, scRNA-seq in human PDAC samples also showed two populations of cancer cells [17]. Subsequent pseudotime trajectory analysis of the mouse PDAC GEMM datasets revealed that expression of Id1 was particularly elevated as malignancy progressed from the early-stage epithelial ductal cell type 1 population to the later-stage ductal cell type 2 mesenchymal-like population (Tang Fan Sci Rep 2022). The same authors analyzed a human scRNA-seq dataset comparing normal pancreas to PDAC and identified ID1 as the top upregulated transcription factor specifically in cancer cells and suggested a role for ID1 in EMT (Tang Fan Sci Rep 2022). Our independent analysis of human scRNA-seq datasets [17] from normal pancreas and PDAC also demonstrated significant upregulation of ID1 expression specifically in the ductal cell type 2 population.

To date there has been little work on the role of BMP signaling in pancreatic exocrine pathogenesis. In support of our finding of the significance of BMP signaling in PDAC, the BMP inhibitor GREM1 was recently identified as a key regulator of cellular heterogeneity in pancreatic cancer. GREM 1 was highly expressed in the mesenchymal 'EPCAM low' tumor cell population where it acted as a paracrine factor to inhibit BMP signaling in epithelial 'EPCAM high' PDAC cells. Inactivation of Grem1 in a PDAC GEMM directly converted epithelial into mesenchymal PDAC while overexpression of Grem1 produced an epithelial phenotype in mesenchymal tumors [34].

With the significance of increased ID1/ID3 expression late in PDAC well-established, it was striking to observe that BMP signaling induced ID1 and ID3 expression as an early event in pancreas pathogenesis. In our experiments, caerulein treatment of wild-type mice, or rat AR42J cells upregulated pSMAD1/5/9 or pSMAD1/5/8 and IDs suggesting that increased BMP signaling had the proposed effect. This finding is consistent with another study that also found high expression of pSMAD1/5/9 in the pancreata of caerulein-treated mice, although the authors did not evaluate expression of ID proteins. These authors went on to show that administration of Noggin to AR42J cells blocked induction of pSMAD1/5/8 and reduced some features of caerulean-induced pancreatitis *in vivo* suggesting a therapeutic effect of inhibiting BMP signaling [35].

An unresolved question is how deletion of SMAD4, which occurs in 50% of PDAC cases as pathogenic cells transition from the PanIN stage to PDAC affects expression of ID1 and ID3. One possibility is that BMP

signaling continues to upregulate IDs through a non-canonical BMP pathway, such as PI3-AKT, which has been proposed by others [10].

Pancreas cancer is projected to become the second leading cause of cancer-related mortality in the U.S. by the year 2030. With more than 90% of cases diagnosed after metastasis has occurred, current treatment regimens result in a relative survival of only 12.5% based on SEER data for 2013-2019. The interaction of ID proteins with bHLH transcription factors has been suggested as a therapeutic target in multiple cancers but the size of the protein-protein interface is relatively large and therefore notoriously difficult to target with small molecules. An alternative strategy may be to identify druggable signaling pathways that impinge on ID1/ID3 expression and/or activity in cancer. BMP signaling is an attractive target for small molecule intervention as it is a highly druggable pathway.

In summary, our findings indicate that BMP signaling to ID proteins is active at each stage of pathogenesis in the exocrine pancreas, providing insight into the etiology of pancreatic maladies.

Materials and Methods

Cell Culture:
Human pancreatic cancer cell lines, PANC-1 and BxPC-3 were cultured in DMEM and RPMI-1640 respectively. Human normal pancreatic cell line, HPNE was cultured in DMEM. 779e PDAC cell line established from patient-derived tumor was a kind gift from A.M. Lowy, M.D. of the Moores Cancer Center, UCSD. All cell lines were purchased from ATCC and were cultured in media supplemented with 10% fetal bovine serum and 100 Units/mL Penicillin/Streptomycin antibiotics (Gibco, Catalog no. 15140-122). All cells were grown in 5% CO_2 at 37°C. 100 ng/mL BMP2 (Peprotech, Catalog no. 120-02C) was added to cells in culture media for 3 hours. 10 uM DMH1 (Fisher Scientific, Catalog no. 501364456) was added to cells in culture media for 24 hours. 200 ng/mL Noggin (Peprotech, Catalog no. 250-38) was added to cells in culture media for 6 hours.

Quantitative RT-PCR:
Total RNA was extracted from drug/vehicle-treated cell lines using NucleoSpin RNA kit (Takara, Catalog no. 740955.50). 2 ug of total RNA extracted was used to synthesize cDNA with qScript Ultra Supermix (Quantabio, Catalog no. 95217). 1 uL of cDNA was used as template for qPCR. Quantitative RT-PCR used CFX96 Touch Real-Time PCR Detection System (BioRad) with PowerUp SYBR Green Master Mix (Applied Biosystems, Catalog No. A25741) with Quantitect human primers (Qiagen) for genes ID1, ID3 and 18S (used for normalization).

Western blots:
Treated cells were lysed in 2X Laemmli buffer (10% β-mercaptoethanol, 20% glycerol, 0.004% bromophenol blue, 0.125 M Tris HCl pH 6.8, 4% sodium dodecyl sulfate) heated for 10 minutes at 100°C followed by centrifugation at 17,000 x g for 15 minutes. Samples were analyzed by sodium dodecyl sulfate–polyacrylamide gel electrophoresis (SDS-PAGE) (4-12% Bis-Tris gel; Bio-Rad Laboratories, Inc.). Gels were transferred to nitrocellulose membranes which were blocked in Intercept blocking buffer (Li-Cor, Catalog no. 927-70001) followed by overnight incubation at 4°C with primary antibodies listed below. Goat anti-

mouse (Li-Cor, IRDye®-800CW RRID:AB_2687553) and goat anti-rabbit (IRDye®-680RD RRID:AB_10974977) secondary antibodies were used at 1:5000 dilution for 1 hour at room temperature. After washes with 1XTBST, membranes were imaged on Licor Odyssey CLX with ImageStudio software. Band intensities were quantified and analyzed by ImageJ.

	Manufacturer (Catalog No.)	Antibody Dilution
Rb-Vinculin	Cell Signaling Technology (13901)	1:1000
Rb-phospho-SMAD1/SMAD5/SMAD8	EMD Millipore Sigma (AB3848-I)	1:1000
Rb-phospho-SMAD1/SMAD5/SMAD9	Abcam (ab92698)	1:1000
Rb-Lamin B1	Abcam (ab16408)	1:1000
Rb-ID3	Cell Signaling Technology (9837S)	1:500
Rb-pHH3	Cell Signaling Technology (9764)	1:1000
E2A (TCF3)	Abcam (ab228699)	1:1000

Immunohistochemistry:

Mouse pancreata were harvested and fixed in 4% PFA. Paraffin embedding, sectioning and slide preparations were done in the SBP Histopathology Core Facility. 5 micron sections on slides were stained on the automated IHC BONDRX (Leica) with the following antibodies: anti-ID3 (Origene, TA500790) with antigen retrieval at pH 6.0 and anti-phospho-SMAD1/SMAD5/SMAD9 (Abcam, ab92698) with antigen retrieval at pH 9.0. Goat anti-rabbit-HRP and goat anti-mouse-HRP was used as secondary antibodies with the BOND polymer refine detection system (Leica, catalog no. DS9800). Images were taken by Zeiss LSM710 confocal microscope with a 10X, 20X and 40X objective lens.

Gene expression comparison:

Microarray datasets including normalized expression levels and metadata from GEO were downloaded in R v4.2.1 using Bioconductor package GEOquery v2.64.2. Gene expression levels were summarized from probe level to gene level by using the median of probes for a given gene. Probes mapped to multiple genes were discarded. Gene expression (RNA-seq) and clinical data from TCGA-PAAD Pan-Cancer 2018 study [36] were downloaded from cBioPortal [37]. Datasets from Cao et al. [16] were downloaded from NCI GDC Data Portal. Tumor versus normal sample comparisons were performed using Wilcoxon rank sum test in R.

Analysis of published scRNA-seq datasets from Ma et al:

Processed count matrices for scRNA-seq datasets from Ma et al. were downloaded from the Gene Expression Omnibus (GEO) database (accession number GSE172380). Low-quality cells were filtered on read counts, the number of genes expressed, and the ratio of mitochondrial reads following the thresholds described in the publication. Filtered gene count matrices were log-normalized, and the top 2000 variable features were further scaled prior to dimension reduction by PCA and being embedded in UMAP using the R package Seurat [38]. Seurat cell clusters were labeled with major cell types using marker genes provided by the authors.

Analysis of published scRNA-seq datasets from Peng et al:

Processed single cell count matrix and cell annotations were downloaded from Genome Sequence Archive under accession PRJCA001063. We used Seurat v4.0.5 for integration and analysis of the data [39]. Raw count matrix and cell metadata were converted to Seurat object. Sample information (tumor or normal) was gleaned from cell barcodes. Raw data was normalized using *NormalizeData* function. Top 2000 highly

variable genes were selected and used for downstream analysis. Data was scaled using *ScaleData*. PCA on highly variable gene set was run using *RunPCA*. Data was integrated using Harmony v0.1.0 [40] based on sample information (tumor and normal samples). *RunUMAP*, *FindNeighbors*, and *FindClusters* functions were to used compute UMAP and cluster the cells using top 40 principal components and resolution of 0.5. Cell types were labelled as described by the original authors [17].

RNA-seq:

PolyA RNA was isolated using the NEBNext® Poly(A) mRNA Magnetic Isolation Module and barcoded libraries were made using the NEBNext® Ultra II™ Directional RNA Library Prep Kit for Illumina® (NEB, Ipswich MA). Libraries were pooled and single end sequenced (1X75) on the Illumina NextSeq 500 using the High output V2 kit (Illumina Inc., San Diego CA).

Bulk RNA-seq analysis:

Raw reads were preprocessed by trimming Illumina Truseq adapters, polyA, and polyT sequences using cutadapt v2.3 (Martin, M. (2011). "Cutadapt removes adapter sequences from high-throughput sequencing reads." EMBnet.journal 17). Trimmed reads were aligned to human genome version hg38 using STAR aligner v2.7.0d_0221 [41] and parameters according to ENCODE long RNA-seq pipeline (https://github.com/ENCODE-DCC/long-rna-seq-pipeline). Gene expression levels were quantified using RSEM v1.3.1 [42]. Ensembl v84 gene annotations were used for the alignment and quantification steps. RNA-seq sequence, alignment, and quantification qualities were assessed using FastQC v0.11.5 (https://www.bioinformatics.babraham.ac.uk/projects/fastqc/) and MultiQC v1.8 [43]. Lowly expressed genes were filtered out by retaining genes with estimated counts (from RSEM) ≥ number of samples times 5. Filtered estimated read counts from RSEM were used for differential expression comparisons using the Wald test implemented in the R Bioconductor package DESeq2 v1.22.2 based on generalized linear model and negative binomial distribution [44]. Genes with Benjamini-Hochberg corrected p-value < 0.05 and fold change ≥ 2.0 or ≤ -2.0 were selected as differentially expressed genes.

Survival analysis:

Survival analysis was performed in R version 4.2.1 using survival, survminer, and maxstat packages. Optimal cutpoints for the categorization of samples as 'high' and 'low' expressors of given gene in each dataset were determined using *surv_cutpoint* and *surv_categorize* functions from survminer package.

Statistical analysis:

Western blot and RT-qPCR data are indicated as Mean ± Standard Deviation. Statistical significance was evaluated by unpaired two-tailed Student's t test. P-values are presented as*p<0.05,**p<0.01,***p<0.001.

References

1. Lee, Y.J., Nam, E.J., Kim, S., Kim, Y.T., Itkin-Ansari, P., and Kim, S.W. (2022). Expression Profiles of ID and E2A in Ovarian Cancer and Suppression of Ovarian Cancer by the E2A Isoform E47. Cancers (Basel) *14*. 10.3390/cancers14122903.
2. Sachdeva, R., Wu, M., Smiljanic, S., Kaskun, O., Ghannad-Zadeh, K., Celebre, A., Isaev, K., Morrissy, A.S., Guan, J., Tong, J., et al. (2019). ID1 Is Critical for Tumorigenesis and

Regulates Chemoresistance in Glioblastoma. Cancer Res *79*, 4057-4071. 10.1158/0008-5472.CAN-18-1357.

3. Kebebew, E., Peng, M., Treseler, P.A., Clark, O.H., Duh, Q.Y., Ginzinger, D., and Miner, R. (2004). Id1 gene expression is up-regulated in hyperplastic and neoplastic thyroid tissue and regulates growth and differentiation in thyroid cancer cells. J Clin Endocrinol Metab *89*, 6105-6111. 10.1210/jc.2004-1234.
4. Swarbrick, A., Roy, E., Allen, T., and Bishop, J.M. (2008). Id1 cooperates with oncogenic Ras to induce metastatic mammary carcinoma by subversion of the cellular senescence response. Proc Natl Acad Sci U S A *105*, 5402-5407. 10.1073/pnas.0801505105.
5. Maruyama, H., Kleeff, J., Wildi, S., Friess, H., Buchler, M.W., Israel, M.A., and Korc, M. (1999). Id-1 and Id-2 are overexpressed in pancreatic cancer and in dysplastic lesions in chronic pancreatitis. Am J Pathol *155*, 815-822. 10.1016/S0002-9440(10)65180-2.
6. Lee, S.H., Hao, E., Kiselyuk, A., Shapiro, J., Shields, D.J., Lowy, A., Levine, F., and Itkin-Ansari, P. (2011). The Id3/E47 axis mediates cell-cycle control in human pancreatic ducts and adenocarcinoma. Mol Cancer Res *9*, 782-790. 10.1158/1541-7786.MCR-10-0535.
7. Kim, S., Lahmy, R., Riha, C., Yang, C., Jakubison, B.L., van Niekerk, J., Staub, C., Wu, Y., Gates, K., Dong, D.S., et al. (2015). The basic helix-loop-helix transcription factor E47 reprograms human pancreatic cancer cells to a quiescent acinar state with reduced tumorigenic potential. Pancreas *44*, 718-727. 10.1097/MPA.0000000000000328.
8. Dufresne, M., Clerc, P., Dieng, M., Edir, A., Couvelard, A., Delisle, M.B., Fourmy, D., and Gigoux, V. (2011). Id3 modulates cellular localization of bHLH Ptf1-p48 protein. Int J Cancer *129*, 295-306. 10.1002/ijc.25668.
9. Tang, Y., Zhang, S., Li, J., Wu, C., and Fan, Q. (2022). ID1 marks the tumorigenesis of pancreatic ductal adenocarcinoma in mouse and human. Sci Rep *12*, 13555. 10.1038/s41598-022-17827-3.
10. Huang, Y.H., Hu, J., Chen, F., Lecomte, N., Basnet, H., David, C.J., Witkin, M.D., Allen, P.J., Leach, S.D., Hollmann, T.J., et al. (2020). ID1 Mediates Escape from TGFbeta Tumor Suppression in Pancreatic Cancer. Cancer Discov *10*, 142-157. 10.1158/2159-8290.CD-19-0529.
11. Shuno, Y., Tsuno, N.H., Okaji, Y., Tsuchiya, T., Sakurai, D., Nishikawa, T., Yoshikawa, N., Sasaki, K., Hongo, K., Tsurita, G., et al. (2010). Id1/Id3 knockdown inhibits metastatic potential of pancreatic cancer. J Surg Res *161*, 76-82. 10.1016/j.jss.2008.10.031.
12. Pei, H., Li, L., Fridley, B.L., Jenkins, G.D., Kalari, K.R., Lingle, W., Petersen, G., Lou, Z., and Wang, L. (2009). FKBP51 affects cancer cell response to chemotherapy by negatively regulating Akt. Cancer Cell *16*, 259-266. 10.1016/j.ccr.2009.07.016.
13. Zhang, G., Schetter, A., He, P., Funamizu, N., Gaedcke, J., Ghadimi, B.M., Ried, T., Hassan, R., Yfantis, H.G., Lee, D.H., et al. (2012). DPEP1 inhibits tumor cell invasiveness, enhances chemosensitivity and predicts clinical outcome in pancreatic ductal adenocarcinoma. PLoS One *7*, e31507. 10.1371/journal.pone.0031507.
14. Sandhu, V., Bowitz Lothe, I.M., Labori, K.J., Lingjaerde, O.C., Buanes, T., Dalsgaard, A.M., Skrede, M.L., Hamfjord, J., Haaland, T., Eide, T.J., et al. (2015). Molecular signatures of mRNAs and miRNAs as prognostic biomarkers in pancreatobiliary and intestinal types of periampullary adenocarcinomas. Mol Oncol *9*, 758-771. 10.1016/j.molonc.2014.12.002.

15. Yang, S., He, P., Wang, J., Schetter, A., Tang, W., Funamizu, N., Yanaga, K., Uwagawa, T., Satoskar, A.R., Gaedcke, J., et al. (2016). A Novel MIF Signaling Pathway Drives the Malignant Character of Pancreatic Cancer by Targeting NR3C2. Cancer Res *76*, 3838-3850. 10.1158/0008-5472.CAN-15-2841.
16. Cao, L., Huang, C., Cui Zhou, D., Hu, Y., Lih, T.M., Savage, S.R., Krug, K., Clark, D.J., Schnaubelt, M., Chen, L., et al. (2021). Proteogenomic characterization of pancreatic ductal adenocarcinoma. Cell *184*, 5031-5052 e5026. 10.1016/j.cell.2021.08.023.
17. Peng, J., Sun, B.F., Chen, C.Y., Zhou, J.Y., Chen, Y.S., Chen, H., Liu, L., Huang, D., Jiang, J., Cui, G.S., et al. (2019). Single-cell RNA-seq highlights intra-tumoral heterogeneity and malignant progression in pancreatic ductal adenocarcinoma. Cell Res *29*, 725-738. 10.1038/s41422-019-0195-y.
18. Bailey, P., Chang, D.K., Nones, K., Johns, A.L., Patch, A.M., Gingras, M.C., Miller, D.K., Christ, A.N., Bruxner, T.J., Quinn, M.C., et al. (2016). Genomic analyses identify molecular subtypes of pancreatic cancer. Nature *531*, 47-52. 10.1038/nature16965.
19. Hingorani, S.R., Wang, L., Multani, A.S., Combs, C., Deramaudt, T.B., Hruban, R.H., Rustgi, A.K., Chang, S., and Tuveson, D.A. (2005). Trp53R172H and KrasG12D cooperate to promote chromosomal instability and widely metastatic pancreatic ductal adenocarcinoma in mice. Cancer Cell *7*, 469-483. 10.1016/j.ccr.2005.04.023.
20. Chakedis, J., French, R., Babicky, M., Jaquish, D., Mose, E., Cheng, P., Holman, P., Howard, H., Miyamoto, J., Porras, P., et al. (2016). Characterization of RON protein isoforms in pancreatic cancer: implications for biology and therapeutics. Oncotarget *7*, 45959-45975. 10.18632/oncotarget.10009.
21. Scully, K.M., Lahmy, R., Signaevskaia, L., Sasik, R., Medal, R., Kim, H., French, R., James, B., Wu, Y., Lowy, A.M., and Itkin-Ansari, P. (2018). E47 Governs the MYC-CDKN1B/p27(KIP1)-RB Network to Growth Arrest PDA Cells Independent of CDKN2A/p16(INK4A) and Wild-Type p53. Cell Mol Gastroenterol Hepatol *6*, 181-198. 10.1016/j.jcmgh.2018.05.002.
22. Hao, J., Lee, R., Chang, A., Fan, J., Labib, C., Parsa, C., Orlando, R., Andresen, B., and Huang, Y. (2014). DMH1, a small molecule inhibitor of BMP type i receptors, suppresses growth and invasion of lung cancer. PLoS One *9*, e90748. 10.1371/journal.pone.0090748.
23. Mohedas, A.H., Xing, X., Armstrong, K.A., Bullock, A.N., Cuny, G.D., and Yu, P.B. (2013). Development of an ALK2-biased BMP type I receptor kinase inhibitor. ACS Chem Biol *8*, 1291-1302. 10.1021/cb300655w.
24. Ejarque, M., Altirriba, J., Gomis, R., and Gasa, R. (2013). Characterization of the transcriptional activity of the basic helix-loop-helix (bHLH) transcription factor Atoh8. Biochim Biophys Acta *1829*, 1175-1183. 10.1016/j.bbagrm.2013.08.003.
25. Hingorani, S.R., Petricoin, E.F., Maitra, A., Rajapakse, V., King, C., Jacobetz, M.A., Ross, S., Conrads, T.P., Veenstra, T.D., Hitt, B.A., et al. (2003). Preinvasive and invasive ductal pancreatic cancer and its early detection in the mouse. Cancer Cell *4*, 437-450. 10.1016/s1535-6108(03)00309-x.
26. Johnson, L., Mercer, K., Greenbaum, D., Bronson, R.T., Crowley, D., Tuveson, D.A., and Jacks, T. (2001). Somatic activation of the K-ras oncogene causes early onset lung cancer in mice. Nature *410*, 1111-1116. 10.1038/35074129.

27. Pan, F.C., Bankaitis, E.D., Boyer, D., Xu, X., Van de Casteele, M., Magnuson, M.A., Heimberg, H., and Wright, C.V. (2013). Spatiotemporal patterns of multipotentiality in Ptf1a-expressing cells during pancreas organogenesis and injury-induced facultative restoration. Development *140*, 751-764. 10.1242/dev.090159.
28. Schlesinger, Y., Yosefov-Levi, O., Kolodkin-Gal, D., Granit, R.Z., Peters, L., Kalifa, R., Xia, L., Nasereddin, A., Shiff, I., Amran, O., et al. (2020). Single-cell transcriptomes of pancreatic preinvasive lesions and cancer reveal acinar metaplastic cells' heterogeneity. Nat Commun *11*, 4516. 10.1038/s41467-020-18207-z.
29. Sah, R.P., Garg, S.K., Dixit, A.K., Dudeja, V., Dawra, R.K., and Saluja, A.K. (2014). Endoplasmic reticulum stress is chronically activated in chronic pancreatitis. J Biol Chem *289*, 27551-27561. 10.1074/jbc.M113.528174.
30. Ma, Z., Lytle, N.K., Chen, B., Jyotsana, N., Novak, S.W., Cho, C.J., Caplan, L., Ben-Levy, O., Neininger, A.C., Burnette, D.T., et al. (2022). Single-Cell Transcriptomics Reveals a Conserved Metaplasia Program in Pancreatic Injury. Gastroenterology *162*, 604-620 e620. 10.1053/j.gastro.2021.10.027.
31. Lerch, M.M., and Gorelick, F.S. (2013). Models of acute and chronic pancreatitis. Gastroenterology *144*, 1180-1193. 10.1053/j.gastro.2012.12.043.
32. Katagiri, T., and Watabe, T. (2016). Bone Morphogenetic Proteins. Cold Spring Harb Perspect Biol *8*. 10.1101/cshperspect.a021899.
33. Kleeff, J., Maruyama, H., Ishiwata, T., Sawhney, H., Friess, H., Buchler, M.W., and Korc, M. (1999). Bone morphogenetic protein 2 exerts diverse effects on cell growth in vitro and is expressed in human pancreatic cancer in vivo. Gastroenterology *116*, 1202-1216. 10.1016/s0016-5085(99)70024-7.
34. Lan, L., Evan, T., Li, H., Hussain, A., Ruiz, E.J., Zaw Thin, M., Ferreira, R.M.M., Ps, H., Riising, E.M., Zen, Y., et al. (2022). GREM1 is required to maintain cellular heterogeneity in pancreatic cancer. Nature *607*, 163-168. 10.1038/s41586-022-04888-7.
35. Cao, Y., Yang, W., Tyler, M.A., Gao, X., Duan, C., Kim, S.O., Aronson, J.F., Popov, V., Takahashi, H., Saito, H., et al. (2013). Noggin attenuates cerulein-induced acute pancreatitis and impaired autophagy. Pancreas *42*, 301-307. 10.1097/MPA.0b013e31825b9f2c.
36. Hoadley, K.A., Yau, C., Hinoue, T., Wolf, D.M., Lazar, A.J., Drill, E., Shen, R., Taylor, A.M., Cherniack, A.D., Thorsson, V., et al. (2018). Cell-of-Origin Patterns Dominate the Molecular Classification of 10,000 Tumors from 33 Types of Cancer. Cell *173*, 291-304 e296. 10.1016/j.cell.2018.03.022.
37. Cerami, E., Gao, J., Dogrusoz, U., Gross, B.E., Sumer, S.O., Aksoy, B.A., Jacobsen, A., Byrne, C.J., Heuer, M.L., Larsson, E., et al. (2012). The cBio cancer genomics portal: an open platform for exploring multidimensional cancer genomics data. Cancer Discov *2*, 401-404. 10.1158/2159-8290.CD-12-0095.
38. Stuart, T., Butler, A., Hoffman, P., Hafemeister, C., Papalexi, E., Mauck, W.M., 3rd, Hao, Y., Stoeckius, M., Smibert, P., and Satija, R. (2019). Comprehensive Integration of Single-Cell Data. Cell *177*, 1888-1902 e1821. 10.1016/j.cell.2019.05.031.
39. Hao, Y., Hao, S., Andersen-Nissen, E., Mauck, W.M., 3rd, Zheng, S., Butler, A., Lee, M.J., Wilk, A.J., Darby, C., Zager, M., et al. (2021). Integrated analysis of multimodal single-cell data. Cell *184*, 3573-3587 e3529. 10.1016/j.cell.2021.04.048.

40. Korsunsky, I., Millard, N., Fan, J., Slowikowski, K., Zhang, F., Wei, K., Baglaenko, Y., Brenner, M., Loh, P.R., and Raychaudhuri, S. (2019). Fast, sensitive and accurate integration of single-cell data with Harmony. Nat Methods *16*, 1289-1296. 10.1038/s41592-019-0619-0.
41. Dobin, A., Davis, C.A., Schlesinger, F., Drenkow, J., Zaleski, C., Jha, S., Batut, P., Chaisson, M., and Gingeras, T.R. (2013). STAR: ultrafast universal RNA-seq aligner. Bioinformatics *29*, 15-21. 10.1093/bioinformatics/bts635.
42. Li, B., and Dewey, C.N. (2011). RSEM: accurate transcript quantification from RNA-Seq data with or without a reference genome. BMC Bioinformatics *12*, 323. 10.1186/1471-2105-12-323.
43. Ewels, P., Magnusson, M., Lundin, S., and Kaller, M. (2016). MultiQC: summarize analysis results for multiple tools and samples in a single report. Bioinformatics *32*, 3047-3048. 10.1093/bioinformatics/btw354.
44. Love, M.I., Huber, W., and Anders, S. (2014). Moderated estimation of fold change and dispersion for RNA-seq data with DESeq2. Genome Biol *15*, 550. 10.1186/s13059-014-0550-8.